CRITICAL SURVEY OF RELATIVISTIC MEAN FIELD APPROACHES

M. Jaminon and C. Mahaux
Institut de Physique B5, Université de Liège, Sart Tilman,
B-4000 Liège 1, Belgium

Abstract. A critical overview is presented of several approaches to the nuclear mean field which share the common feature of claiming that the Dirac equation is more appropriate than the Schrödinger equation for the description of the average nucleon-nucleus interaction. The discussion bears on the Dirac phenomenology, renormalizable Lagrangian models, the relativistic Brueckner-Hartree-Fock approximation and the relativistic impulse approximation. Emphasis is deliberately put on open problems rather on successes.

1. INTRODUCTION

The last few years have witnessed the appearance of a continuously increasing flux of papers which suggest that the existence of "large Lorentz scalar and vector components of the baryon self-energy are genuine features of the nuclear many-body problem"[1]) and that, consequently, "the nucleus is best treated as a relativistic system"[2]). The implications of this belief are sufficiently important to require a critical examination of the solidity of the "growing body of evidence that relativistic effects may play a more important role in the description of nuclear phenomena than previously thought"[3]).

The present paper is an attempt in that direction. Our presentation is admittedly unbalanced since we deliberately put emphasis on open problems rather than on available answers. We hope that this is acceptable since most surveys[1,4,5,6]), including one of our own[7]), rather adopt a positive optimistic attitude, which is also necessary for pursuing the development of these drastically novel approaches.

One of the difficulties encountered when attempting this critical evaluation is that the relativistic approaches may be quite different from one another despite the existence of several common features. Therefore it is sometimes unjustified to consider that a success of one relativistic approach supports the assumptions made in another one. In the following discussion the various approaches are ordered according to their remoteness from models of the nucleon-nucleon interaction; this also roughly corresponds to an historical ordering. Section 2 thus deals with the Dirac phenomenology, sect. 3 with renormalizable Lagrangian models, sect. 4 with the relativistic Brueckner-Hartree-Fock approximation, sects. 5 and 6 with a relativistic impulse approximation for nucleon-nucleus and antinucleon-nucleus scattering and sect. 7 to a

relativistic impulse approximation based on a boson-exchange model for the nucleon-nucleon interaction. Section 8 contains our conclusions.

2. PHENOMENOLOGICAL DIRAC ANALYSES

The Dirac phenomenology consists in using the Dirac equation ($\hbar = c = 1$)

$$[\vec{\alpha}.\vec{p} + \gamma^o(m + U^D)]\Psi^D = (\varepsilon + m)\,\Psi^D \qquad (2.1)$$

for the analysis of nucleon-nucleus scattering. Here, ε denotes the bombarding energy and m the nucleon mass. The Dirac optical-model potential $U^D = V^D + i\,W^D$ is a 4×4 matrix. We consider a doubly-closed shell symmetric target nucleus. One can without any restriction limit oneself to local potentials[8]. The Dirac potential can then be written as the sum of four Lorentz components, namely[9]

$$U^D(r) = U^D_s(r) + \gamma^o\,U^D_o(r) + \gamma^r\,U^D_v(r) - i\,\gamma^o\gamma^r\,U^D_t(r) \quad , \qquad (2.2)$$

where γ^r is the radial γ-matrix.

The Dirac OMP (2.2) involves four unknown complex functions. We now argue that only two of these can be determined by phenomenological analyses of the elastic scattering cross sections. The reasoning is the following. Let $w_{\ell j}(r;\varepsilon)$ denote the radial part of the large components of the spinor $\Psi^{D\ell j}$ after a partial wave decomposition. It is always possible to find a function $g(r)$ which approaches a constant for $r \to 0$ and unity for $r \to \infty$, and which is such that the function $v_{\ell j}(r) = g(r)\,w_{\ell j}(r)$ fulfills the Schrödinger-type equation

$$\frac{d^2}{dr^2}\,v_{\ell j}(r) + \{k_\infty^2 - \frac{\ell(\ell+1)}{r^2} - 2m[U^{Se}_{cent}(r;\varepsilon) - U^{Se}_{so}(r;\varepsilon)\,K_{\ell j}]\}\,v_{\ell j}(r) = 0 \ , \qquad (2.3)$$

where $K_{\ell j}$ is equal to $-(j + 3/2)$ if $j = \ell - \frac{1}{2}$ and to $(j - \frac{1}{2})$ if $j = \ell + \frac{1}{2}$, while $k_\infty^2 = (\varepsilon + m)^2 - m^2$ is the square of the relativistic asymptotic momentum. Furthermore, it can be shown that the elastic scattering cross section and the polarization observables can be calculated from the phase shift associated with $v_{\ell j}$ by using the usual formulas[7,10]. It is because of this property that $U^{Se}(r;\varepsilon)$ plays a privileged role as compared to operators which appear in other two-component reductions (compare with ref.[11])) and can be called the "Schrödinger-equivalent potential"[10,12].

Innumerable nonrelativistic analyses show that it is possible to fit the experimental data by adjusting the two functions $U^{Se}_{cent}(r;\varepsilon)$ and $U^{Se}_{so}(r;\varepsilon)$ which appear in the nonrelativistic equation (2.3). One should therefore expect that good fits can be also obtained from the Dirac phenomenology by adjusting only two of the four Lorentz components of the Dirac potential U^D. Correspondingly it is not surprizing that good fits to the experimental data can be obtained from a Dirac phenomenological analysis even if one sets equal to zero two of the Lorentz components of $U^D(r;\varepsilon)$. In practically all previous analyses the two quantities $U^D_v(r)$ and $U^D_t(r)$ have a priori been dropped. In this "S-V" (Scalar-Vector) model the real parts of the two remaining components, namely $V^D_s(r;\varepsilon)$ (the "scalar" component) and $V^D_o(r;\varepsilon)$ (the "vector" component) are assumed to have a Woods-Saxon shape. It is then found from the analyses that in the nuclear interior V^D_s is large and negative ($\approx$ - 400 MeV) while V^D_o is large and positive ($\approx$ + 300 MeV). The reason is that U^{Se}_{cent} involves the sum $V^D_o + V^D_s$, while the spin-orbit strength U^{Se}_{so} involves the difference $V^D_s - V^D_o$. The empirical value of the spin-orbit coupling requires that the values of $|V^D_s|$ and of $|V^D_o|$ must both be large in the phenomenological S-V model. Therefore the relativistic effects are large in this model, even for low energy nucleons. For instance, the small components of the plane wave spinor Ψ^D in nuclear matter are enhanced by a factor $m/(m + V^D_s) \approx 2$ as compared to their value in free space[13]).

One must, however, remain aware that from a purely phenomenological point of view no reason exists for assuming that U^D_v and U^D_t vanish. We now show that good fits to the data can be obtained with a Dirac "S-T" optical-model potential in which $U^D_o = U^D_v = 0$, while U^D_s and U^D_t differ from zero but are both small. We only consider real potentials, for simplicity. We assume the following shapes : $V^D_s(r) = V_s\ f(r)$, $V^D_t(r) = (V_{to}/m)\ (df(r)/dr)$, where $f(r) = [1 + \exp(r-R)/b]^{-1}$, with values of R and b typical of ^{40}Ca. The upper part of Fig. 1 shows (for $\varepsilon = 0$) the dependence upon V_{to} of the depth of the central part of the Schrödinger-equivalent potential and of the surface value of its spin-orbit part. The depth of $V^{Se}_{cent}(r=0.1\ fm)$ is quite insensitive to the value of V_{to}. The empirical value of $V^{Se}_{so}(r=R)$ as given by Becchetti and Greenlees[14]) is reproduced for $V_{to} \approx$ - 200 MeV, which corresponds to $V^D_t(R) = \delta \approx 20$ MeV at the nuclear surface. The lower part of Fig. 1 shows the radial dependence of the spin-orbit part V^{Se}_{so} of this Schrödinger-equivalent potential.

This discussion corroborates a previous study by Miller[9]). It confirms that the experimental data (elastic scattering cross sections, single-particle energies) at low energy are compatible with small va-

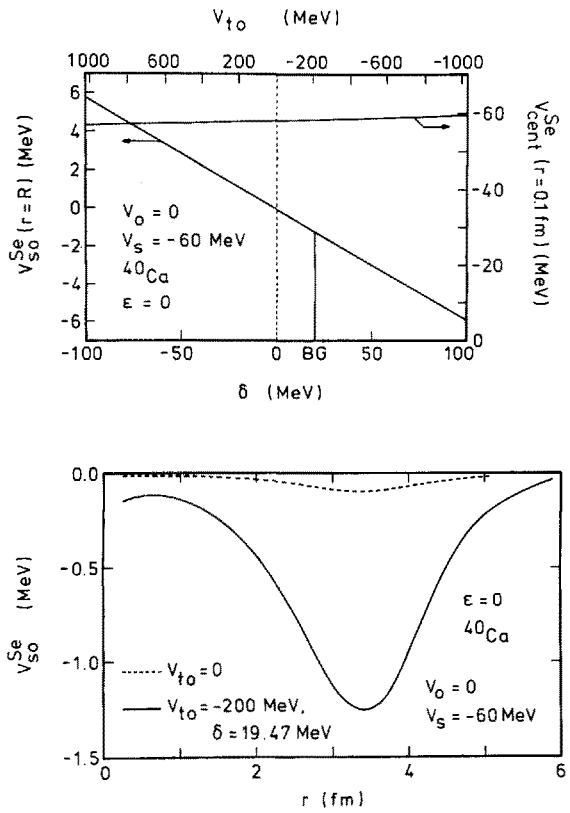

Fig. 1. The upper drawing shows the dependence upon the strength V_{to} of the Dirac tensor potential of the depth of the central part (right-hand ordinate scale) and of the surface value of the spin-orbit part (left-hand ordinate scale) of the Schrödinger-equivalent potential for zero bombarding energy, in the case of a phenomenological S-T Dirac potential in which the vector potential vanishes while the scalar potential has a Woods-Saxon shape (typical of ^{40}Ca) with a depth equal to - 60 MeV . The value labelled BG reproduces the strength of the empirical spin-orbit coupling at the nuclear surface. The lower drawing gives the radial dependence of the spin-orbit part of the Schrödinger-equivalent potential in the case of this S-T model, for $V_{to} = 0$ (dashes) and $V_{to} = -200$ MeV (full curve).

lues of the Lorentz components. Note, however, that the single-particle wavefunctions calculated from the S-V model on the one hand and from the S-T model on the other hand can be quite different in the nuclear interior. However, it is quite difficult to find experimental data which are sensitive to the internal part of the single-particle wavefunction and whose theoretical interpretation is unambiguous.

Let us give a second example of the freedom which exists in constructing a phenomenological Dirac optical-model potential. Let Ψ^D denote the Dirac spinor associated with a scalar-vector (S-V) model, i.e. *in a model in which* $U_v^D = U_t^D = 0$. Clark et al.[3]) have recently introduced the transformation $\Phi^D = e^{\gamma_o F(r)} \Psi^D$ and shown that the quantity $F(r)$ can be chosen in such a way that Φ^D is a solution of a Dirac equation with $U_{o1} = U_{v1} = 0$, i.e. corresponds to a S-T (Scalar-Tensor) model; the index 1 labels this new model. The function $F(r)$ approaches unity for large r , and the S1-T1 model is therefore phase shift equivalent to the original S-V model. Both models moreover yield the same bound state energies.

For illustration, we consider the example of a phenomenological

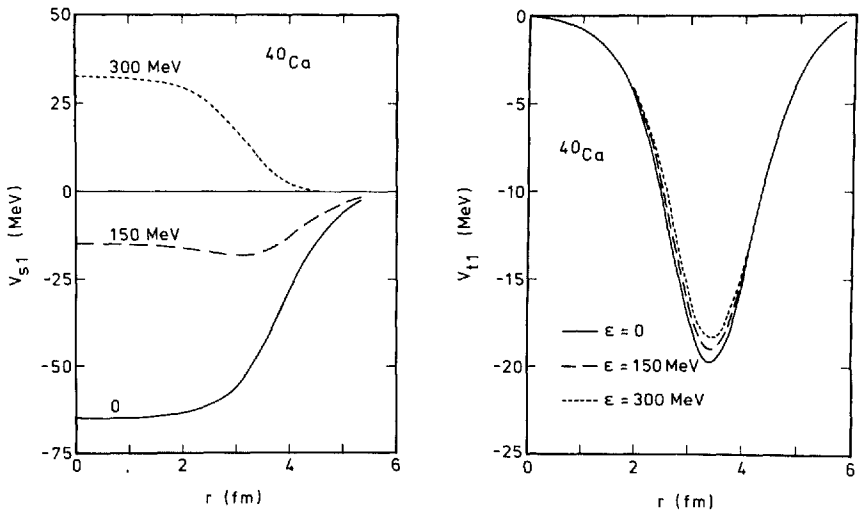

Fig. 2. Radial dependence for bombarding energies equal to 0 , 150 and 300 MeV of the real parts of the scalar (left-hand side) and of the tensor (right-hand side) Lorentz components of a scalar-tensor (S-T) model which is phase-shift equivalent to a scalar-vector (S-V) model in which the scalar and vector Lorentz components both have the same Woods-Saxon shape (with geometrical parameters corresponding to ^{40}Ca), with potential depths equal to V_s = - 400 Mev and V_o = + 300 MeV , respectively.

S-V model which yields good agreement with the p-^{40}Ca cross section at 200 MeV ; the potential depths are given by V_s = - 400 MeV , V_o = + 300 MeV [3]).

The real parts V_{s1} and V_{t1} of the scalar and tensor potentials in the corresponding S-T model are shown in Fig. 2. It is seen that the two Lorentz components are quite weak, in contrast to the Lorentz components V_s^D and V_o^D of the original S-V model. We have obtained[15]) an analytical proof of the observation[3]) that the associated S-V and S-T models yield exactly the same Schrödinger-equivalent potential. This property is likely to be a consequence of an inverse scattering theorem. It supports our opinion that the Schrödinger-equivalent potential is a very useful reference potential. We note, however, that the S-T and S-V models are only phase shift equivalent. The corresponding wavefunctions Φ^D and Ψ^D are different in the nuclear interior. For instance the two models yield different predictions for the magnetic moment of nuclear ground states[16]).

We conclude from this discussion that phenomenological analyses of nucleon-nucleus scattering and of single-particle energies cannot demonstrate the necessity of replacing the nonrelativistic optical model by a relativistic one. The phrasing of this sentence reflects the critical point of view that we deliberately adopt. Indeed, we could have well concluded that phenomenological analyses cannot exclude the possi-

bility that large relativistic effects exist. Moreover, it should be added that the analyses yield good fits with potential shapes which are simpler in the scalar-vector than in the scalar-tensor model[3]).

3. RENORMALIZABLE LAGRANGIAN MODELS

The relativistic quantum field models are based on a Lagrangian density which contains field operators associated with hadrons (mesons and nucleons), whence the expression "quantum hadrodynamics" (QHD) coined for this approach[1]). The Lagrangian models are required to be renormalizable in order to provide a systematic way of evaluating observables.

The parameters which appear in the Lagrangian density (meson masses, coupling constants) are not directly related to those which characterize physical mesons nor with those which are introduced in boson-exchange models for the free nucleon-nucleon interaction. Rather these parameters should be considered as "effective" : they are chosen in such a way that the measured values of some observables are reproduced by the solution of the model within some approximation scheme. They should be readjusted when the approximation scheme is changed.

Let us consider the example of symmetric nuclear matter and of the σ-ω model originally developed by Walecka[17]). The corresponding Lagrangian density is

$$\mathcal{L} = g_\sigma \bar{\psi} \varphi_\sigma \psi - g_\omega \bar{\psi} \gamma^\mu \omega_\mu \psi \quad , \tag{3.1}$$

where ψ refers to the nucleon field and φ_σ , ω_μ to neutral scalar and vector meson fields, respectively. The fields obey nonlinear coupled equations; one of these reads

$$[\gamma^\mu(i\partial_\mu - g_\omega\omega_\mu) - (m - g_\sigma\varphi_\sigma)]\psi = 0 \quad . \tag{3.2}$$

Walecka's mean field approximation consists in replacing in this equation the operators ω_μ and φ_σ by their expectation value with respect to a Fermi sea. Equation (3.2) then yields the following equation for the plane wave spinor $\psi = u(\vec{q})\exp(i\vec{q}.\vec{r})$:

$$[\vec{\alpha}.\vec{q} + \gamma^o(m + V_s + \gamma^o V_o)]u(\vec{q}) = (\varepsilon + m)\, u(\vec{q}) \quad . \tag{3.3}$$

Here,

$$(\epsilon + m - V_o)^2 = q^2 + (m + V_s)^2 \quad , \tag{3.4a}$$

$$V_o = \rho\, g_\omega^2/m_\omega^2 \quad , \quad V_s = -\rho_s\, g_\sigma^2/m_\sigma^2 \quad , \tag{3.4b}$$

$$\rho = \sum_{q<k_F} u^+(\vec{q})\, u(\vec{q}) \quad , \quad \rho_s = \sum_{q<k_F} u^+(\vec{q})\, \gamma^o\, u(\vec{q}) \quad , \tag{3.4c}$$

while k_F denotes the Fermi momentum. The scalar density ρ_s is smaller than the baryon density ρ because the squares of the small components of $u(\vec{q})$ appear with different signs in ρ and ρ_s. The average binding energy per nucleon is given by

$$B/A = \langle T \rangle + \tfrac{1}{2} \langle V \rangle \quad , \tag{3.5a}$$

where

$$\langle T \rangle = 3\, k_F^{-3} \int_o^{k_F} u^+(\vec{q})\, [\vec{\alpha}.\vec{q} + \gamma^o\, m]\, u(\vec{q})\, q^2\, dq - m \quad , \tag{3.5b}$$

$$\langle V \rangle = 3\, k_F^{-3} \int_o^{k_F} u^+(\vec{q})\, \gamma^o\, [V_s + \gamma^o\, V_o)]\, u(\vec{q})\, q^2\, dq \quad . \tag{3.5c}$$

Equations (3.5a-c) are typical of a model in which the nucleons only feel the average potential created by the other nucleons. It is therefore not surprizing that one can develop relativistic Hartree and Hartree-Fock approximations in which eqs. (3.3) and (3.5a-c) also hold. The outcomes of the latter two approximations are represented by the full and the dashed curves in the upper part of Fig. 3, for a common set of input parameters. The lower part of Fig. 3 shows that in each case the input parameters can be adjusted in such a way as to yield the empirical saturation point of symmetric nuclear matter.

One characteristic feature of eq. (3.3) is that the spinor $u(\vec{q})$ depends upon V_s, which in turn depends upon $u(\vec{q})$ via ρ_s. This implies a self-consistent calculation. It also indicates that $\langle T \rangle$ is not equal to the average kinetic energy per nucleon of a noninteracting Fermi gas (it even becomes negative for large k_F), in contradistinction with the case of the nonrelativistic Hartree, Hartree-Fock or Brueckner-Hartree-Fock approximation.

The small value of the average binding energy per nucleon results from a sizeable cancellation between the contributions of the scalar and vector Lorentz components V_s and V_o, which both have a large absolute magnitude (several hundreds MeV). The size of the difference between the results of the relativistic Hartree and Hartree-Fock approximations is typical of the size (about ten per cent) of several corrections to the Hartree approximation which have been evaluated until

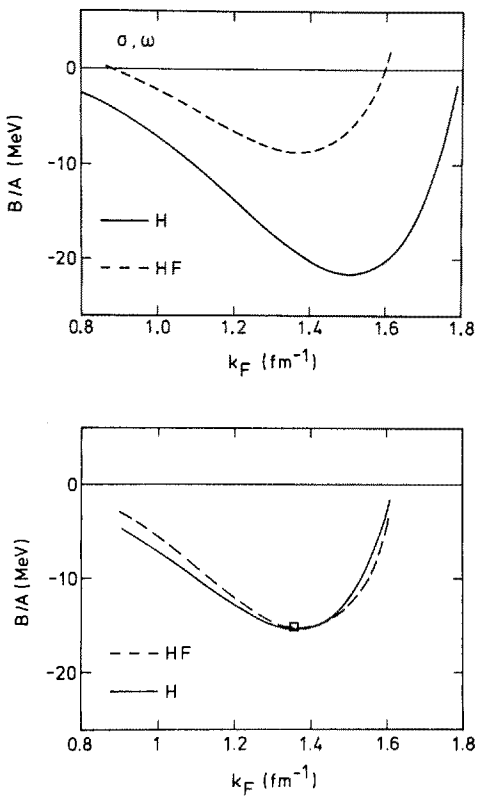

Fig. 3. Adapted from refs. [4,18]*. The upper drawing represents the dependence upon the Fermi momentum* k_F *of the average binding energy per nucleon of symmetric nuclear matter, for the input parameters adopted by Brockmann* [19]*; the full curve corresponds to the Hartree (mean field) approximation and the dashes to the Hartree-Fock approximation. The lower part shows that in both cases the input parameters can be adjusted in such a way as to reproduce the empirical saturation point, which is represented by an open square.*

now, see e.g. ref.[20]).

This relative insensitivity has been considered as indicating that the existence of "large Lorentz scalar and vector components are genuine features of the nucleon many-body problem"[1]). Caution must however be excercised. Indeed, this conclusion is derived from the schematic model (3.1) for the Lagrangian density. Moreover, it appears that in all the approximation schemes the average binding energy per nucleon is given by an expression which involves an integration over the nucleon momenta from 0 to k_F, as on the right-hand side of eqs. (3.5b,c). This indicates that these approximation schemes assume that the Fermi sea is not depleted. In nonrelativistic calculations the depletion of the Fermi sea is found to be as large as ten to twenty per cent, mainly because of short-range and tensor correlations[21]). It would be of great interest to evaluate the depletion in the case of the relativistic Lagrangian models.

Progress is being made towards the inclusion of other types of meson fields in the Lagrangian density[1]). However, it will remain difficult to evaluate to what extent these models are realistic since they involve a fairly large number of adjustable parameters, while the fit-

ted bulk properties of nuclei only depend upon a rather small number of quantities. This difficulty is associated with the fact that in these approaches contact is lost with free nucleon-nucleon scattering, for which several thousands observables have been measured.

An important test of these relativistic quantum field models and of the approximation schemes would probably consist in confronting with experiment their predictions concerning the behaviour of antinucleons in a nuclear medium. In the case of the Lagrangian model (3.1) and of the mean field approximation it appears likely that the scalar and vector potentials add constructively in the Schrödinger-equivalent potential for antinucleons, whose depth would then reach about - 700 MeV . This seems to be at variance with recent empirical observations on the antiproton-nucleus interaction. It is not clear whether the blame should be put on the model Lagrangian, on the approximation scheme or both.

4. RELATIVISTIC BRUECKNER-HARTREE-FOCK APPROXIMATION

The relativistic Brueckner-Hartree-Fock approximation was initiated by the Brooklyn group[6]). It has been improved in refs.[20,22,23]). The corresponding expression of the average binding energy per nucleon has the same form as in eq. (3.5a). Now, however, $\langle V \rangle$ is the expectation value of a relativistic Brueckner reaction matrix M, which fulfills the Bethe-Goldstone equation

$$M = V + V(Q/e)\, M \quad ; \tag{4.1}$$

here, V is the sum of the irreducible contributions to the kernel of the Bethe-Salpeter equation for free nucleon-nucleon scattering and $(1/e)$ is an energy propagator, while

$$Q = \sum_{a,b>k_F} |\vec{a}\rangle|\vec{b}\rangle \langle\vec{a}|\langle\vec{b}| \tag{4.2}$$

is the Pauli exclusion operator which requires the intermediate momenta to be larger than the Fermi momentum.

The dash-and-dot curve in Fig. 4 shows the results originally obtained by the Brooklyn group. They are in good agreement with the empirical location of the saturation point and derive from a cancellation between large scalar and vector Lorentz components in the nucleon self-energy. This original cancellation suffers from the use of an obsolete nucleon-nucleon potential V and from the use of free plane wave spinors for the intermediate states $|\vec{a}\rangle$ and $|\vec{b}\rangle$. A more modern version

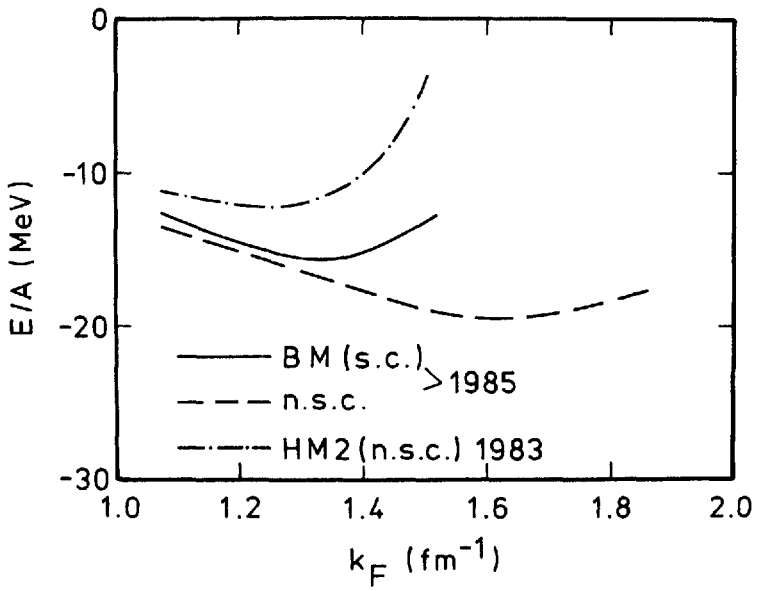

Fig. 4. Dependence upon the Fermi momentum k_F of the average binding energy per nucleon in nuclear matter, as calculated from the relativistic Brueckner-Hartree-Fock approximation. The dash-one dot curve has been obtained by the Brooklyn group[6]) from a free nucleon-nucleon potential previously constructed by Holinde and Machleidt (HM2, ref.[24])), taking free plane wave spinors in the expression of the Pauli operator Q and free energies e_a, e_b in the propagator $(e)^{-1}$. The full curve has recently been evaluated by Machleidt and Brockmann[23]), who used a more modern expression for V and self-consistent prescriptions for the spinors $|\vec{a}\rangle$, $|\vec{b}\rangle$ and for the propagator $(e)^{-1}$ which appear in eqs. (4.1), (4.2). The long dashes show how the full curve is modified if these self-consistent prescriptions are relaxed.

of V yields the long dashes and the use of self-consistent prescriptions for $|\vec{a}\rangle$, $|\vec{b}\rangle$ and $(1/e)$ gives the solid line in Fig. 4 [23]). This result is in excellent agreement with the empirical saturation properties. This is puzzling. Indeed the difference between the full and the dashed lines in Fig. 4 shows the quantitative importance of the self-consistent prescriptions. However the latter have not been fully justified. The self-consistent choice of the propagator $(1/e)$ is a matter of debate even in the nonrelativistic Brueckner-Hartree-Fock approximation. This can hardly be envisaged in the relativistic case since the basic Lagrangian is probably not renormalizable. Some corrections should nevertheless be studied, for instance the one associated with the depletion of the Fermi sea.

The nucleon-nucleus optical-model potential evaluated by the Brooklyn group in the framework of the Brueckner-Hartree-Fock approximation is in fair agreement with the empirical one[6]). It would be of interest to check that this agreement is not affected by the use of a modern free nucleon-nucleon interaction V and of self-consistent prescrip-

tions. For intermediate energies it would also be useful to study the difference between the Brueckner-Hartree-Fock approximation and the impulse approximation.

The results of the relativistic Brueckner-Hartree-Fock approximation only differ from those of the Hartree-Fock approximation by about ten per cent. It appears that the experimental data on antinucleon-nucleus scattering may request a much larger difference between the relativistic Hartree-Fock and Brueckner-Hartree-Fock approximations. It would thus be of great interest to extend the relativistic Brueckner-Hartree-Fock approximation to the case of antinucleons.

5. RELATIVISTIC IMPULSE APPROXIMATION

While the relativistic Brueckner-Hartree-Fock approximations uses as input a model for the free nucleon-nucleon potential operator V, the relativistic impulse approximation is based on the transition matrix for free nucleon-nucleon scattering. In refs.[25-27]), the following two relations have been adopted for defining a relativistic transition operator F^D:

$$\bar{u}_1(\vec{q}_1',s_1')\,\bar{u}_2(\vec{q}_2',s_2')\,F^D\,u_1(\vec{q}_1,s_1)\,u_2(\vec{q}_2,s_2)$$

$$= \chi_1^+(\vec{q}_1',s_1')\,\chi_2^+(\vec{q}_2',s_2')\,F^S\,\chi_1(\vec{q}_1,s_1)\,\chi_2(\vec{q}_2,s_2) \quad , \tag{5.1}$$

$$F^D = F_s + F_v\,\gamma_1^\mu\,\gamma_{2\mu} + F_t\,\sigma_1^{\mu\nu}\,\sigma_{2\mu\nu} + F_a\,\gamma_1^5\,\gamma_1^\mu\,\gamma_2^5\,\gamma_{2\mu} + F_{ps}\,\gamma_1^5\,\gamma_2^5 \, . \tag{5.2}$$

Here, $\chi(\vec{p},s)$ denotes a two-component Pauli free plane wave spinor, F^S be the corresponding nonrelativistic transition operator as determined from free nucleon-nucleon scattering data, and $u(\vec{p},s)$ be a four-component Dirac free plane wave spinor.

The original impulse approximation to the relativistic optical-model potential essentially consists in taking the expectation value of F^D with respect to the target ground state approximated by a Slater determinant built with four-component Dirac spinors. It turns out[25]) that the corresponding relativistic optical-model potential has large scalar and vector Lorentz components, and that these are in good agreement with those derived from phenomenological Dirac analyses based on the S-V model. The full curve in Fig. 5 shows that the agreement is particularly spectacular in the case of the ratio of the depths of these two Lorentz components; this ratio is the quantity believed to be most accurately determined by phenomenological analyses of the expe-

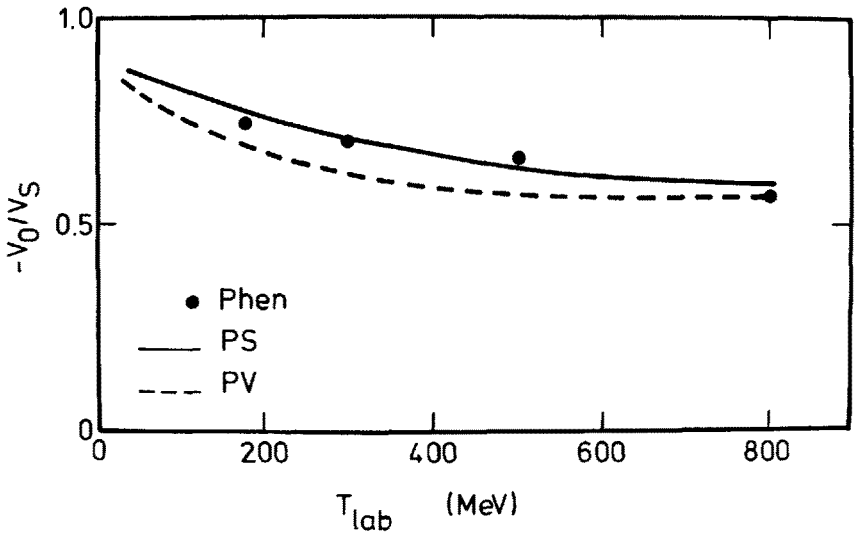

Fig. 5. Energy dependence of the modulus of the ratio between the depths of the vector and scalar Lorentz components of the relativistic optical-model potential. The full dots are empirical values derived from phenomenological analyses based on the Dirac scalar-vector model[26]). The full curve is obtained from the impulse approximation based on eqs. (5.1) and (5.2)[25]). The dashed curve has been computed from the dashed lines in Fig. 9 below, i.e. from another version of the impulse approximation, which essentially amounts to replacing the exchange operator associated with a pseudoscalar π-N coupling by that associated with a pseudovector π-N coupling[29]).

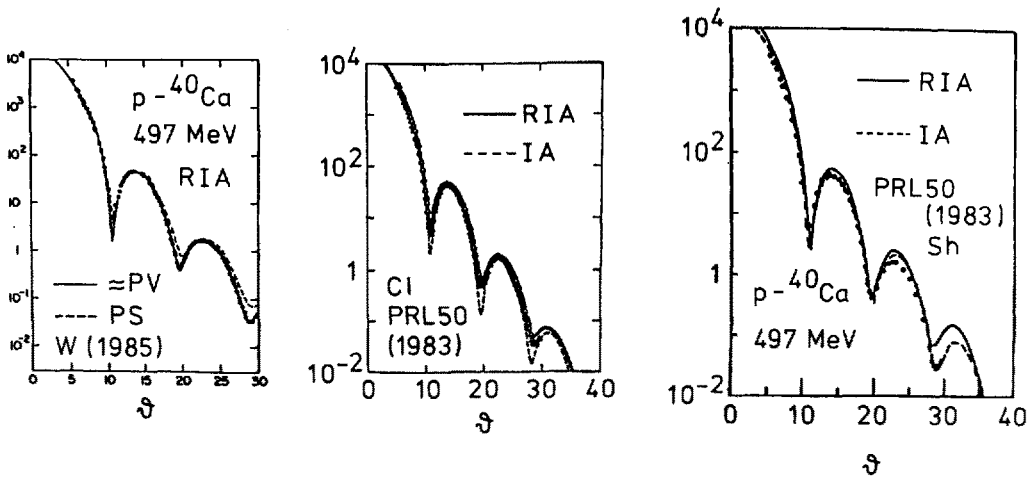

Fig. 6. Dependence upon scattering angle of the differential cross section (in mb/sr) for the elastic scattering of 497 MeV protons by ^{40}Ca. The dots are empirical values. The dashed curves and the full curves have been calculated from nonrelativistic and relativistic (eqs. (5.1), (5.2)) impulse approximations by the authors of ref.[27]) (middle drawing) and of ref.[26]) (right-hand side), respectively. The dashed curve on the left-hand side should also correspond to this relativistic impulse approximation, while the full curve is based on a modified version which essentially amounts to assuming a pseudovector rather than a pseudoscalar π-N coupling.

rimental data.

The full curves in the middle and right-hand parts of Fig. 6 show the differential cross sections predicted by the relativistic impulse approximation in the case of the scattering of 500 MeV protons by ^{40}Ca, as computed by two different groups. They are both in good agreement with the data but differ from one another. These groups also give different results for the nonrelativistic impulse approximation. The origin of these differences should be made clear if one wants to attach a quantitative significance to the difference between the nonrelativistic and the relativistic impulse approximations. One may also wonder why the corrections to the relativistic impulse approximation should be very small, for instance those due to the correlations in the target. One must also keep in mind that the impulse approximation involves the neutron distribution, which is not accurately known. It also seems that it has not been justified why the corresponding potential can be used in connection with a Dirac single-particle wave equation.

The relativistic impulse approximation yields a very good agreement between calculated and measured spin observables (analyzing power, spin rotation function). This is quite impressive since no parameter has been adjusted. However, a parameter free model is not an assumption free theory. In the present context, it has been pointed out by Adams and Bleszynski[30]) that the prescription (5.2) for defining F^D is largely arbitrary. The origin of this ambiguity essentially is that there exists an infinite number of ways of writing a matrix operator F^D which fulfills eq. (5.1). Physically this is related to the fact that F^S describes the scattering between two positive energy nucleons, while a full specification of F^D would also involve the description of nucleon-antinucleon scattering. Moreover the impulse approximation requires off-the-energy shell extrapolations of the nucleon-nucleon scattering amplitudes, and this is not provided by the nucleon-nucleon scattering data.

6. ANTINUCLEON-NUCLEUS POTENTIAL

The main characteristic of the relativistic quantum field models is that they involve degrees of freedom which are associated with antiparticles. Hence it appears essential to investigate to what extent these models account for the recent data on antiproton-nucleus scattering. It turns out that the impulse approximation outlined in the preceding section is quite successful in that respect[31]). The real and imaginary parts of the corresponding Schrödinger-equivalent potential

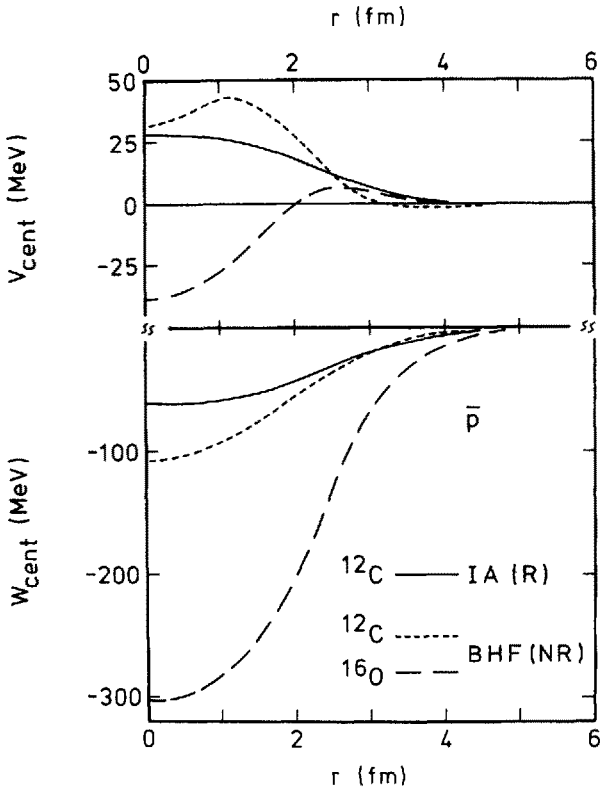

Fig. 7. Taken from ref.[32]). Real (top) and imaginary (bottom) parts of the calculated nonrelativistic optical-model potentials for 46.8 MeV antiprotons on ^{12}C (full curve and short dashes) and for 0 MeV antiprotons on ^{16}O (long dashes). The short dashes[33,34]) correspond to the nonrelativistic Brueckner-Hartree-Fock approximation and the full curves[31]) to the relativistic impulse approximation (sect. 5); both calculations are based on the same free nucleon-antinucleon amplitudes[35]). The long dashes[36]) are computed from the nonrelativistic Brueckner-Hartree-Fock approximation with a different input for the nucleon-antinucleon potential operator[37]).

are represented by the full curves in Fig. 7. As in the nucleon case it results from a cancellation between large scalar and vector Lorentz components. These have opposite signs, in contrast to what would apparently be the case in the relativistic Hartree approximation. This suggests that the Lorentz structure of the free nucleon-antinucleon potential operator may be quite different from that of the nucleon-antinucleon scattering amplitude.

Figures 7 and 8 exhibit that the nonrelativistic Brueckner-Hartree-Fock approximation yields approximately the same results as the relativistic impulse approximation. The agreement with experimental data is quite good in both cases. This is somewhat puzzling since none of these approximations takes into account the existence of correlations among the target nucleons. The answer probably lies in the property that the antiprotons are strongly absorbed, so that elastic scattering only occurs in the tail of the nuclear surface.

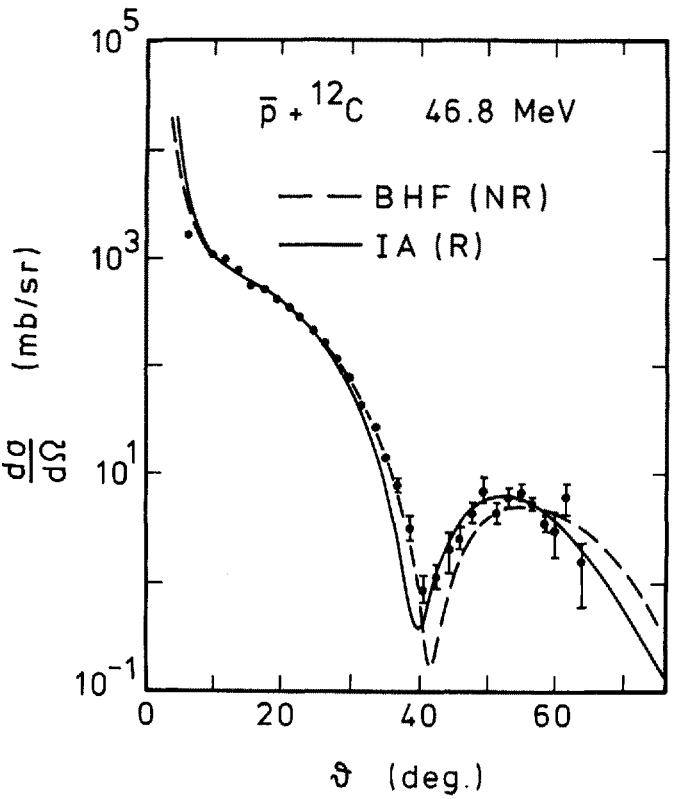

Fig. 8. Taken from ref.[32]). Differential cross section for the elastic scattering of 46.8 MeV antiprotons by ^{12}C. The dots are empirical values[38]). The full curve and the long dashes have been calculated from the optical-model potentials represented in Fig. 7 with the same notation.

7. MESON EXCHANGE AND THE RELATIVISTIC IMPULSE APPROXIMATION

The relativistic impulse approximation discussed in sect. 5 uses as input the free nucleon-nucleon scattering amplitudes, which as mentioned are insufficient for uniquely specifying the "relativistic" transition operator F^D in eq. (5.1). This arbitrariness can only be waived if a theoretical model is constructed for F^D. This problem has recently been attacked by Tjon and Wallace, and by Horowitz[29,39-41]). These authors first identified the origin of the fact that the relativistic impulse of sect. 5 yields vector and scalar potentials which have an extremely large magnitude at low energy, see the full curves in Fig. 9. They then argued that this could be avoided by a suitable modification of assumption (5.2), and that this modification finds support in boson-exchange models of the nucleon-nucleon interaction provided that one uses a pseudovector pion-nucleon coupling.

Tjon and Wallace obtain the scalar and vector strengths represented by the dashed curves in Fig. 9; their ratio yields the dashed curve

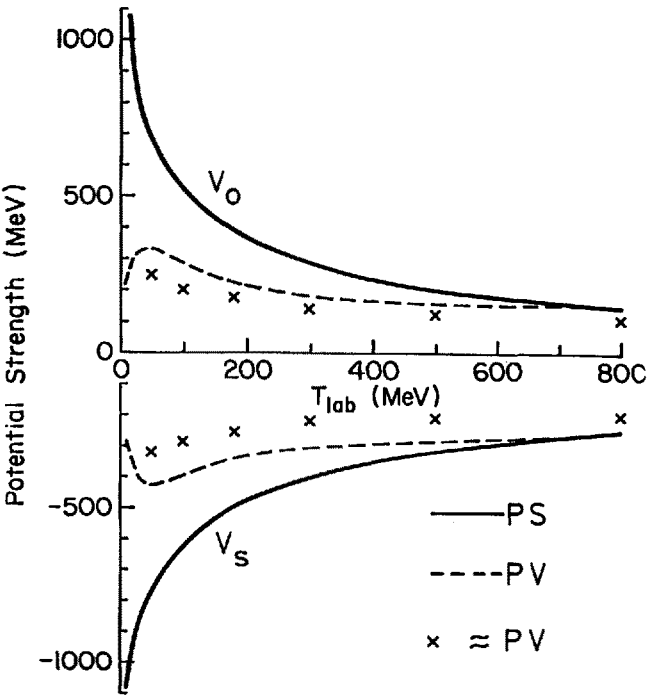

Fig. 9. From refs.[29,40]). Energy dependence of the strengths of the scalar (V_s) and vector (V_o) Lorentz components of the nucleon self-energy in nuclear matter as evaluated from the relativistic impulse approximation. The full curves correspond to the version outlined in sect. 5; their ratio yields the full curve shown in Fig. 5. The long dashes are associated with a modification of the assumption (5.2); they agree with results (crosses) derived from the Bethe-Salpeter equation for free nucleon-nucleon scattering when a pseudovector instead of pseudoscalar coupling is used for the pion-nucleon vertex.

shown in Fig. 5. Above 200 MeV the calculated ratio is seen to be in less good agreement with the empirical value than the one which had previously been found from assumption (5.2), but this feature seems to be reversed below 200 MeV [40]). It is not clear to what extent this is really significant since medium Pauli and binding energy corrections are expected to become sizeable below 200 MeV . A crucial test of these meson exchange approaches to F^D would consist in testing their predictions concerning antinucleon-nucleon and antinucleon-nucleus scattering.

8. DISCUSSION

We first summarize some of the main problems encountered in the relativistic approaches. The Dirac phenomenology (sect. 2) requires assumptions on the Lorentz structure of the optical-model potential; the size of the relativistic effects drastically depends upon the assumption which is adopted. The renormalizable quantum field models (sect. 3) are not yet able to include some of the most important meson fields; even if they could, the number of adjustable parameters would be too large for allowing their determination from the nuclear data, unless

one can establish contact with free nucleon-nucleon scattering. The relativistic Brueckner-Hartree-Fock approximation (sect. 4) and the relativistic impulse approximation (sects. 5-7) yield very good agreement with empirical data; this raises the problem of explaining why the corrections to these approximations should be small; these corrections are delicate to treat since the models are not renormalizable. It would be of great interest to evaluate the depletion of the Fermi sea : could it be that it is smaller in some relativistic approaches because strong short-range nucleon-nucleon correlations do not appear ? Could one test this experimentally ? Much attention should also be devoted to the antinucleon-nucleon and antinucleon-nucleus cases, since the appearance of antiparticle degrees of freedom is one of the main characteristics of a relativistic quantum field theory.

We have mainly focused on nucleon-nucleus scattering, which only probes the single-particle wavefunction at large distance. The enhancement of the small components of the wavefunction which is typical of the relativistic approaches only exists in the nuclear interior, where it is quite difficult to experimentally probe the wavefunction. For instance the expression of the coupling between the nucleons and an electromagnetic field is ambiguous in the relativistic approaches[42]). This is related to the problem of embedding the internal structure of the nucleons in the relativistic models. To what extent a Dirac equation could be consistent with the composite structure of the nucleons is an interesting problem[43]).

Finally, we must recall that here we have deliberately adopted a critical attitude, and thereby have not given a balanced presentation of the various relativistic approaches. We have adopted the view that the field deserves a critical survey precisely because of the great interest that it justifiably raises. Real advances are usually initiated by bold assumptions, and one should not let oneself be hindered by difficulties. It appears safe to perform a translation in time and adopt the same conclusion as in the paper that we had presented exactly six years ago in this very same room, namely :"Many problems remain to be solved and intriguing questions are raised by the apparent success of the relativistic approaches. This should give rise to a flurry of activity in the near future"[10]).

REFERENCES

1. B.D. Serot and J.D. Walecka, in Advances in Nuclear Physics, vol. 16, J.W. Negele and E. Vogt, eds. (Plenum Press, 1985)
2. C.M. Shakin, Brooklyn City College preprint 84/093/131
3. B.C. Clark, S. Hama, S.G. Kälbermann, E.D. Cooper and R.L. Mercer, Phys.Rev. **C31** (1985) 694

4. M. Jaminon and C. Mahaux, **in** New Horizons in Electromagnetic Physics, J.V. Noble and R.R. Whitney, eds. (University of Virginia, Charlottesville, 1983), p. 108
5. B.C. Clark, S. Hama, S.G. Kälbermann, E.D. Cooper and R.L. Mercer, **in** Neutron-Nucleus Collisions. A Probe of Nuclear Structure, J. Rapaport, R.W. Finlay, S.M. Grimes and F.S. Dietrich, eds. (American Institute of Physics, New York, 1985) p. 123
6. M.R. Anastasio, L.S. Celenza, W.S. Pong and C.M. Shakin, Phys.Reports **100** (1983) 327
7. M. Jaminon, Ph.D. Thesis (Liège, 1982)
8. L.D. Miller, Phys.Rev. **C12** (1975) 710
9. L.D. Miller, Ann.Phys. (N.Y.) **91** (1975) 40
10. M. Jaminon, C. Mahaux and P. Rochus, Phys.Rev. **C22** (1980) 2027
11. E.D. Cooper, A.O. Gattone and M.H. Macfarlane, J.Phys. **G9** (1983) L131
12. M. Jaminon, C. Mahaux and P. Rochus, Phys.Rev.Lett. **43** (1979) 1097
13. M. Jaminon and C. Mahaux, **in** Recent Progress in Many-Body Theories, J.G. Zabolitzky, M. de Llano, M. Fortes and J.W. Clark, eds. (Springer Verlag, 1981), p. 60
14. F.D. Becchetti and G.W. Greenlees, Phys.Rev. **182** (1969) 1190
15. M. Jaminon and C. Mahaux, unpublished
16. M. Bawin and G.L. Strobel, to be published
17. J.D. Walecka, Ann.Phys. (N.Y.) **83** (1974) 491
18. M. Jaminon, C. Mahaux and P. Rochus, Nucl.Phys. **A365** (1981) 371
19. R. Brockmann, Phys.Rev. **C18** (1978) 1510
20. C.J. Horowitz and B.D. Serot, Phys.Lett. **137B** (1984) 287
21. S. Fantoni and V.R. Pandharipande, Nucl.Phys. **A427** (1984) 473
22. R. Brockmann and R. Machleidt, Phys.Lett. **149B** (1984) 283
23. R. Machleidt and R. Brockmann, **in** Proceedings of the 1984 LAMPF Workshop on Dirac Approaches to Nuclear Physics (to be published)
24. K. Erkelenz, Phys.Reports **13** (1974) 191
25. J.A. McNeil, J.R. Shepard and S.J. Wallace, Phys.Rev.Lett. **50** (1983) 1439
26. J.R. Shepard, J.A. McNeil and S.J. Wallace, Phys.Rev.Lett. **50** (1983) 1443
27. B.C. Clark, S. Hama, R.L. Mercer, L. Ray and B.D. Serot, Phys.Rev.Lett. **50** (1983) 1644
28. B.C. Clark and R.L. Mercer, quoted in ref.[25])
29. J.A. Tjon and S.J. Wallace, Phys.Rev. C (in press)
30. D.L. Adams and M. Bleszynski, Phys.Lett. **136B** (1984) 10
31. B.C. Clark, S. Hama, J.A. McNeil, R.L. Mercer, L. Ray, B.D. Serot, D.A. Sparrow and K. Stricker-Bauer, Phys.Rev.Lett. **53** (1984) 1423
32. M. Jaminon and C. Mahaux, **in** Proceedings of the 1985 Trieste Conference on Perspectives in Nuclear Physics at Intermediate Energies (World Scientific Publ.Comp. Singapore, in press)
33. H.V. Von Geramb, K. Nakano and L. Rikus, preprint (1984)
34. H.V. Von Geramb, **in** Neutron-Nucleus Collisions. A Probe of Nuclear Structure, J. Rapaport, R.W. Finlay, S.M. Grimes and F.S. Dietrich, eds. (American Institute of Physics, New York, 1985) p. 14
35. J. Côté, M. Lacombe, B. Loiseau, B. Moussalam and R. Vinh Mau, Phys.Rev.Lett. **48** (1982) 1319
36. T. Suzuki and H. Narumi, Nucl.Phys. **A426** (1984) 413
37. R.A. Bryan and R.J.N. Phillips, Nucl.Phys. **B5** (1968) 201
38. D. Garretta et al., Phys.Lett. **135B** (1984) 266
39. J.A. Tjon and S.J. Wallace, Phys.Rev.Lett. **54** (1985) 1357
40. S.J. Wallace, **in** Proceedings of the 1985 LAMPF Workshop on Dirac Approaches to Nuclear Physics (to be published)
41. C.J. Horowitz, Phys.Rev. **C31** (1985) 1340
42. T. de Forest, Jr., Phys.Rev.Lett. **53** (1984) 895
43. S.J. Brodsky, Comments Nucl.Part.Phys. **12** (1984) 213.